A small-molecule activator of kinesin-1 drives remodeling of the microtubule network

Thomas S. Randall[a], Yan Y. Yip[a], Daynea J. Wallock-Richards[a], Karin Pfisterer[a], Anneri Sanger[a], Weronika Ficek[a], Roberto A. Steiner[a], Andrew J. Beavil[a], Maddy Parsons[a], and Mark P. Dodding[a,b,1]

[a]Randall Centre for Cell and Molecular Biophysics, King's College London, London SE1 1UL, United Kingdom; and [b]School of Biochemistry, University of Bristol, Bristol BS9 1TD, United Kingdom

Edited by Eva Nogales, University of California, Berkeley, CA, and approved November 21, 2017 (received for review August 25, 2017)

The microtubule motor kinesin-1 interacts via its cargo-binding domain with both microtubules and organelles, and hence plays an important role in controlling organelle transport and microtubule dynamics. In the absence of cargo, kinesin-1 is found in an autoinhibited conformation. The molecular basis of how cargo engagement affects the balance between kinesin-1's active and inactive conformations and roles in microtubule dynamics and organelle transport is not well understood. Here we describe the discovery of kinesore, a small molecule that in vitro inhibits kinesin-1 interactions with short linear peptide motifs found in organelle-specific cargo adaptors, yet activates kinesin-1's function of controlling microtubule dynamics in cells, demonstrating that these functions are mechanistically coupled. We establish a proof-of-concept that a microtubule motor–cargo interface and associated autoregulatory mechanism can be manipulated using a small molecule, and define a target for the modulation of microtubule dynamics.

kinesin-1 | microtubule dynamics | kinesore | small molecule | intracellular transport

The heterotetrameric kinesin-1 microtubule motor plays a crucial role in spatial organization of many subcellular components by virtue of its capacity to transport diverse protein and ribonuclear protein complexes, vesicles, and organelles on microtubules (1–4). Kinesin-1 also regulates the organization of the microtubule network itself, through its ability to mediate microtubule–microtubule interactions that result in their bundling and sliding (5–9). This activity is important for cytoplasmic streaming in *Drosophila* oocytes, formation of microtubule-based cellular processes, and axonal regeneration (5, 10). These diverse functions rely on a capacity to translocate with high processivity toward the plus end of microtubules imparted by the microtubule binding amino terminal ATPase motor domains of the dimeric kinesin heavy chains (KHCs) and a multivalent cargo-binding domain comprised of the C-terminal domains of the KHCs and the kinesin light chains (KLCs), which contain binding sites for both organelle-specific cargo adaptors and microtubules (9, 11–15).

In the absence of cargo, kinesin-1 is in an autoinhibited, folded conformation that is stabilized by the interaction of a single C-terminal KHC tail with the motor domain dimer interface, thereby cross-linking the two motor domains and preventing futile cycles of ATP hydrolysis (16–22). We have recently shown that the KLCs, which regulate kinesin-1 activity (23, 24), also engage *in cis* in a second autoinhibitory intramolecular interaction between their tetratricopeptide repeat domain (KLC^{TPR}) and a negatively charged unstructured linker region immediately preceding it, carrying a leucine-phenylalanine-proline (LFP) motif (25). Binding of organelle-specific cargo adaptors containing "W-acidic" short linear-peptide motifs to KLC^{TPR}, which can initiate kinesin-1 activation (11, 26, 27), displaces this intramolecular interaction causing a conformational change within the KLCs (25). We proposed that this cargo-dependent conformational change acts a molecular switch to control the activity of the holoenzyme (25). We also recently provided evidence to suggest that one consequence of W-acidic motif engagement of KLC^{TPR} is to make a cargo-binding site in the KHC tail that is inaccessible in the autoinhibited conformation, available to bind cargo (28). The predominantly basic series of amino acids comprising this site can interact with closely related cargo-adaptor sequences to stabilize the kinesin-1–cargo interaction and, interestingly, is also known to interact with microtubules in an ATP-independent manner (9, 14, 15, 19). Collectively, these data suggest a stepwise model for kinesin-1 activation, in which engagement of KLC^{TPR} and the resulting light-chain conformational change is the key upstream signal to activate kinesin-1 and, in a context-dependent manner, results in either organelle transport—if KHC interacts with an organelle cargo adaptor (28)—or microtubule bundling and sliding, if KHC interacts with microtubules. In support of such a proposition, the KLCs have been demonstrated to modulate the affinity of the KHC-tail for microtubules in a manner dependent upon the KLC LFP-acidic linker region (24), and the W-acidic motif containing kinesin-1 adaptor calsyntenin-1 was recently shown to play a role in regulating microtubule organization in dendritic arbor development (29). One prediction of such a model is that if kinesin-1 were to be activated under conditions where its capacity to interact with organelles was limited, its role in microtubule sliding and bundling would be promoted.

We employed a chemical biology-based approach to test this hypothesis, seeking to identify small molecules that could induce KLC^{TPR}-dependent kinesin-1 activation in the absence of organelle cargo-adaptor engagement. This resulted in the identification of a compound that we have named kinesore, which in vitro inhibits the interaction of KLC^{TPR} with the W-acidic lysosomal cargo adaptor SKIP. We show that in cells, kinesore induces the light-chain conformational switch in a similar manner to activating cargo and causes the large-scale kinesin-1–

Significance

Herein we identify kinesore as a cell permeable small-molecule modulator of the kinesin-1 microtubule motor. Kinesore acts through the cargo-binding domain of the motor to activate its function in controlling microtubule dynamics. Our chemical biology approach to understanding microtubule motor protein function provides mechanistic insight into how this poorly understood activity of kinesin-1 is regulated and establishes a proof-of-concept that a microtubule motor–cargo interface and associated autoregulatory mechanism can be manipulated using a small molecule. In doing so, we define a target for the modulation of microtubule dynamics. We suggest that this offers a conceptual approach to consider for the chemical manipulation of the cytoskeleton and its motor proteins.

Author contributions: T.S.R., Y.Y.Y., D.J.W.-R., A.J.B., M.P., and M.P.D. designed research; T.S.R., Y.Y.Y., D.J.W.-R., K.P., W.F., and M.P.D. performed research; A.S. contributed new reagents/analytic tools; T.S.R., Y.Y.Y., R.A.S., M.P., and M.P.D. analyzed data; and M.P.D. wrote the paper.

The authors declare no conflict of interest.

This article is a PNAS Direct Submission.

[1]To whom correspondence should be addressed. Email: mark.dodding@bristol.ac.uk.

This article contains supporting information online at www.pnas.org/lookup/suppl/doi:10.1073/pnas.1715115115/-/DCSupplemental.

dependent remodeling of the microtubule network. Thus, we demonstrate that the organelle transport and microtubule sliding/bundling functions of the motor are coupled through a shared activation mechanism. Moreover, we establish a proof-of-concept that a microtubule motor–cargo interface and associated autoregulatory mechanism can be manipulated using a small molecule, and offer an unexpected target for the modulation of microtubule dynamics.

Results

Identification of Kinesore as a Small-Molecule Inhibitor of the KLC2–SKIP Interaction. To identify small molecules that could induce KLC^{TPR}-dependent kinesin-1 activation in the absence of organelle cargo-adaptor engagement, we focused on the interaction between autoinhibited $aiKLC2^{TPR}$ (KLC2 161–480, previously designated $KLC2^{extTPR}$) and a W-acidic motif peptide from the lysosomal cargo-adaptor SKIP ($SKIP^{WD}$) (25). Inclusion of the autoinhibitory N-terminal sequence on $KLC2^{TPR}$ results in an approximate eightfold reduction in binding affinity (K_D increases to ∼8 μM from ∼1 μM). To bind $KLC2^{TPR}$, $SKIP^{WD}$ displaces this autoinhibitory interaction (25). Thus, one possible mechanism for the small-molecule–mediated inhibition of the SKIP–$aiKLC2^{TPR}$ interaction would be for a compound to act in a similar fashion to SKIP by displacing the intramolecular interaction to occupy the SKIP binding site, thus potentially mimicking SKIP-induced activation while simultaneously inhibiting SKIP binding. This formed the rationale for a high-throughput small-molecule screen.

We developed a primary in vitro time-resolved (TR) FRET assay (Fig. 1*A*, *Top*) coupled to a secondary fluorescence polarization (FP) -based assay (Fig. 1*A*, *Middle*) to identify compounds that had the capacity to inhibit the interaction between $aiKLC2^{TPR}$ and $SKIP^{WD}$ and screened the 2,908 compound Chemogenomic Library provided by Pfizer (see *Materials and Methods* for details). A tertiary FP screen of compounds from the Hit-2-Lead library (Chembridge), informed by this dataset, resulted in the identification of 3,5-dibromo-N′-{[2,5-dimethyl-1-(3-nitrophenyl)-1H-pyrrol-3-yl] methylene}-4-hydroxybenzohydrazide, hereafter named "kinesore" (Fig. 1*A*, *Bottom*).

Consistent with its ability to target the kinesin-1–cargo interface, in pull-down assays, kinesore inhibited the interaction between purified recombinant GST-SKIP (1–310) and full-length hemaglutinin (HA)-KLC2 with a 50% reduction in binding at 12.5 μM and elimination of any detectable binding at a 25 μM kinesore (Fig. 1*B*). In FP assays, kinesore inhibited the interaction of $TAMRA\text{-}SKIP^{WD}$ with $aiKLC2^{TPR}$ in a concentration-dependent manner (Fig. 1*C*) (30). Based upon this activity profile, and penetrant cellular phenotype described below, we decided to pursue it further. To the best of our knowledge, this compound has not been characterized before in any other context.

Kinesore Remodels the Microtubule Network. To examine the effect of kinesore in cells, HeLa cells were treated with 50 μM kinesore for 1 h. As SKIP mediates the kinesin-1–dependent transport of late endosomes (LE)/lysosomes on microtubules (31), cells were immunostained for β-tubulin and LAMP1 (LE/lysosomes). In control conditions, as expected, lysosomes were distributed throughout the cytoplasm, with some peripheral and perinuclear clusters, in association with the characteristic radial microtubule array typically observed in this cell type (Fig. 2*A*, *Upper*). Remarkably, in kinesore-treated cells, the microtubule network was entirely reorganized into a series of loops and bundles (Fig. 2*A*, *Lower*). In addition, the lysosomal compartment accumulated in a juxtanuclear position, where there were relatively few microtubules. At 50 μM kinesore, this phenotype was highly penetrant, with 95 ± 2.4% (n = 3, total of 200 cells) of cells exhibiting a reorganized nonradial microtubule network. This phenotype emerged progressively with prominent loops and bundles in most cells becoming apparent after 30–35 min of treatment (Fig. S1). In titration experiments, in cells treated for 1 h, this phenotype became apparent at a concentration of 25 μM kinesore, with relatively little effect at or below concentrations of 12.5 μM (Fig.

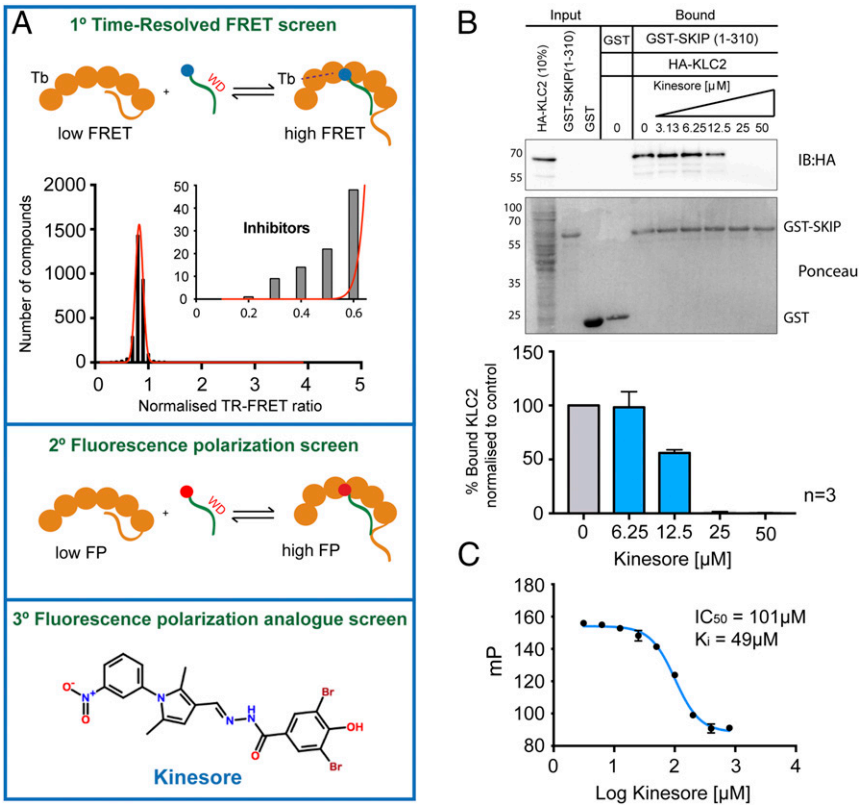

Fig. 1. Identification of kinesore as a small-molecule inhibitor of KLC–cargo interaction. (*A*) Scheme showing three-stage screening strategy for small molecule inhibitors of the $aiKLC2^{TPR}$–$SKIP^{WD}$ (SEQ: STNLEWDDSAI) interaction and the chemical structure of kinesore. (*B*) Western blot of GST pull-down experiment showing that the interaction between bacterially expressed GST-SKIP (1–310) and HA-KLC2 expressed in mammalian cell extracts is inhibited by kinesore. All pull-down lanes, including controls were performed in the presence of 0.1% DMSO. Graph shows quantification of three independent experiments. Error ± SEM (*C*) FP experiment titrating increasing concentrations of kinesore into a $aiKLC2^{TPR}$:$SKIP^{WD}$ complex showing that kinesore inhibits the interaction. Data are derived from three replicates and are representative of three independent experiments. Error ± SEM.

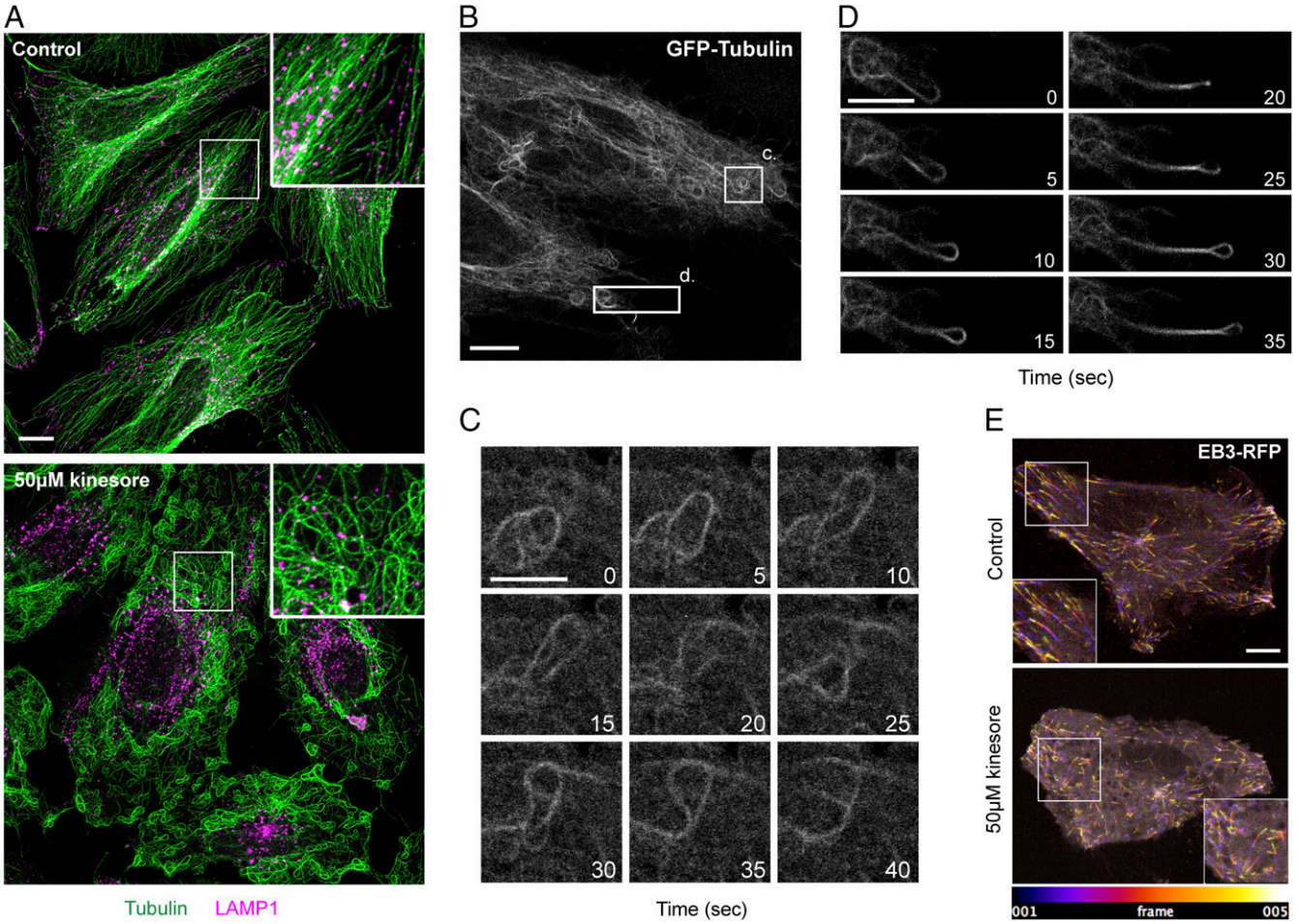

Fig. 2. Kinesore induces the remodeling of the microtubule network. (*A*) Representative maximum-intensity projection immunofluorescence images acquired using a Ziess 880 Airyscan microscope of HeLa cells treated with 50 μM kinesore or vehicle control (0.1% DMSO) for 1 h. Cells were immunostained for β-tubulin (green) and LAMP1 (magenta). (Scale bar in *A,* 10 μm. Enlargement magnification: 2.6×.) (*B–D*) Stills derived from Movie S1 showing representative dynamics of GFP-tubulin in live HeLa cells treated with 50 μM kinesore for 1 h. Numbering denotes time in seconds from start of the still sequence. (Scale bars: *B,* 10 μm; *C* and *D,* 5 μm.) (*E*) Pseudocolored spinning-disk confocal microscopy projection images from the first five frames (20 s) of Movies S2 and S3, showing dynamics of EB3-RFP in control and kinesore-treated HeLa cells. (Scale bar in *E*: 10 μm. Enlargement magnification: 1.5×.)

S2*A*). The effect was reversible because a 2-h washout of kinesore from cells treated for 1 h led to the reestablishment of the radial microtubule array (Fig. S2*B*), suggesting that this effect was not due to acute toxicity of the compound.

To examine the dynamic behavior of the reorganized microtubule network, HeLa cells stably expressing GFP–α-tubulin were treated with kinesore for 1 h and imaged live. This revealed that the loops/bundles of microtubules, particularly in the cell periphery, were highly dynamic and engaged in complex microtubule–microtubule interactions (Fig. 2 *B* and *C* and Movie S1). This phenotype is highly reminiscent of cells that overexpress the microtubule sliding *Drosophila* kinesin-14 family motor, Ncd, and so we considered this to be consistent with our hypothesis (32). Occasionally, cells also extended microtubule-based projections (Fig. 2*D* and Movie S1). Treatment of cells stably expressing the plus-end binding protein EB3 fused to red fluorescent protein (RFP) showed that while microtubule plus-ends remained highly dynamic, the spatial organization and directionality of EB3 comets appeared disordered compared with control cells (Fig. 2*E* and Movies S2 and S3). Treatment of cells with 10 μM nocodazole disrupted kinesore induced loops and bundles (Fig. S3).

This kinesore-induced reorganization of the microtubule network was observed in a panel of mammalian normal and cancer cell lines, and thus was not restricted to HeLa cells (Fig. S4). To our knowledge, this cellular phenotype does not closely resemble that of any known microtubule-targeting agents that act directly upon tubulin, and consistent with this, kinesore did not significantly affect the kinetics of microtubule assembly in in vitro polymerization reactions and microtubules polymerized in the presence of kinesore were equally susceptible to cold-induced destabilization (Fig. S5).

Kinesore-Induced Remodeling of the Microtubule Network Is Dependent on Kinesin-1. Next, we examined the effect of kinesore on cells overexpressing kinesin-1. In control cells transfected with Citruline (mCit)-tagged KHC (Kif5C) and HA-tagged KLC (KLC2), which form a complex when overexpressed (28), kinesin-1 displayed a predominantly diffuse localization and the microtubule network appeared substantially normal (Fig. 3*A*, *Left*). Consistent with an activation-like effect upon kinesin-1, in kinesore-treated cells, KHC and KLC accumulated at the cell periphery (Fig. 3*A*, *Right*). In addition, the morphology of the kinesore-remodeled microtubule network was altered. Intracellular loops were less prominent, but instead cells showed large numbers of microtubule-rich projections emanating from the cell periphery. Structured illumination microscopy (SIM) imaging confirmed that kinesin-1 (KHC and KLC) associated with tubulin at the cell periphery in kinesore-treated cells (Fig. 3*B*). We also noted their accumulation at the tip of a subset of microtubule-rich projections (Fig. 3*B*). Collectively, these data

suggest that, as kinesore alters the localization of kinesin-1, and high expression of kinesin-1 modifies the kinesore-microtubule phenotype, kinesore likely acts upon kinesin-1. Consistent with this, fluorescent protein-labeled kinesin-1 subunits expressed under control of their endogenous promoter in HeLa-Kyoto cells (33), which display a predominantly diffuse localization under control conditions, associated with kinesore-induced microtubule loops and bundles (Fig. S6). Similarly, when these cells (GFP-Kif5B) were lysed in a microtubule-stabilizing buffer, kinesore increased the amount of KHC associated with a microtubule-containing pellet fraction following sedimentation (Fig. S7) without affecting the amount of tubulin in the pellet.

Formally testing the kinesin-1–dependence of kinesore-induced remodeling of microtubules is complicated by the multiple genes that can encode KHC (*Kif5A, Kif5B, Kif5C*) and KLC (*KLC1, KLC2, KLC3, KLC4*), which have distinct cell- and tissue-expression profiles and which have the potential to undergo compensatory changes in expression following loss of a specific isotype (34). To address this, we used the commercially available KHC (KIF5B) CRISPR knockout, chronic myeloid leukemia-derived HAP1 cell line, and matched wild-type control. In wild-type HAP1 cells, transcriptomic data suggest that Kif5B is the predominant isotype at 61 transcripts per million. Kif5C is present at 21 transcripts per million while Kif5A is not expressed (35). Consistent with this, Kif5B was detected in wild-type cell extracts using a Kif5B-specific polyclonal antibody, but was absent in Kif5B KO cells. In contrast, pan-KHC antibody revealed a substantial but not complete reduction in total KHC expression, suggesting the presence of lower levels of another isotype (Fig. 3*C*). In wild-type cells, 50 μM kinesore induced the remodeling of the microtubule network and the formation of extensive microtubule-rich projections. This phenotype was strongly suppressed in Kif5B knockout cells, confirming that microtubule remodeling induced by kinesore is dependent upon the presence of kinesin-1.

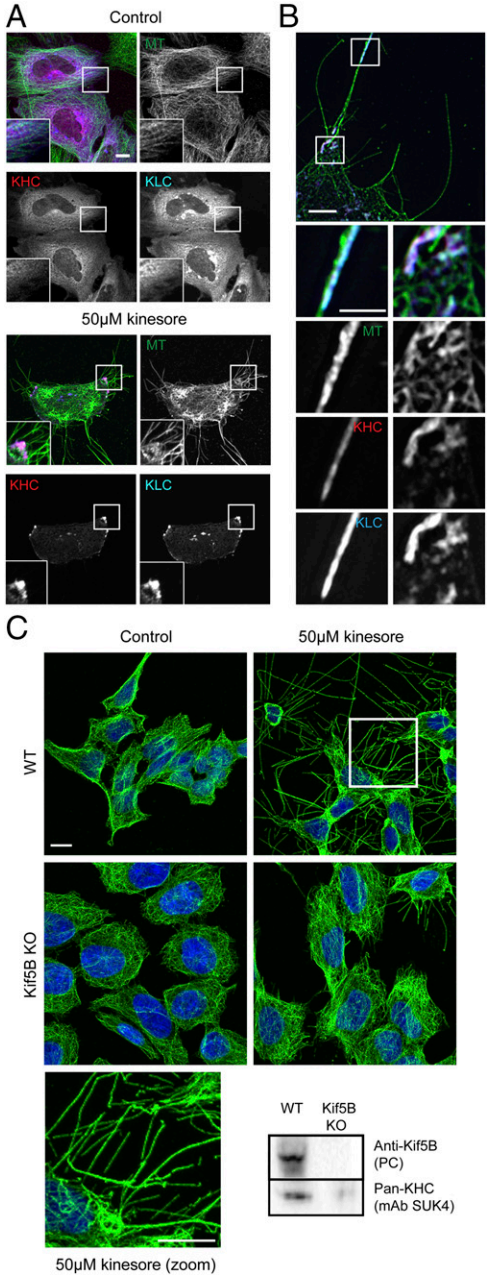

Fig. 3. Kinesore-induced remodeling of the microtubule network is dependent on kinesin-1. (*A*) Representative maximum-intensity projection confocal immunofluorescence images showing HeLa cells transfected with mCit-KHC (pseudocolored red) and HA-KLC (pseudocolored blue) treated with 50 μM kinesore (*Right*) or vehicle control (*Left*) (0.1% DMSO) for 1 h. Note the change in localization of kinesin-1 (KHC/KLC) and formation of microtubule-rich projections in kinesore-treated cells. Images are representative of three independent experiments (Scale bar, 10 μm. Enlargement magnification: 2.9×.) (*B*) Structured illumination images of kinesore-treated cells as in *A*. (Scale bar in *B*, 5 μm; 2.5 μm in enlargement.) (*C*) Representative immunofluorescence images of HAP1 cells (wild-type or Kif5B knockout) treated with 50 μM kinesore or vehicle control (0.1% DMSO) for 1 h and stained for β-tubulin (green) or DNA (Hoechst, blue). Microtubule-rich projections induced by kinesore are strongly suppressed by knockout of Kif5B. (Scale bar, 10 μm.) Western blot shows whole-cell extracts of wild-type or Kif5B knockout HAP1 cells probed with either a Kif5B specific polyclonal antibody or a pan-KHC monoclonal antibody (SU.K.4).

Kinesore Induces the Light-Chain Conformational Switch. These data suggest that kinesore, by engaging the KLC^{TPR} in a manner that inhibits interactions of kinesin-1 with activating cargo adaptors, may act in a "cargo-mimetic" manner to promote kinesin-1 activation. To test this hypothesis, we employed our previously validated KLC conformation biosensor (Fig. 4*A*) (25). In the absence of exogenous cargo, this biosensor reports a high FRET state consistent with a compact KLC conformation (FRET efficiency 15.77 ± 0.76%). FRET is reduced by coexpression of the cytoplasmic domain of the W-acidic cargo adaptor CSTN1 (5.82 ± 1.02%) (Fig. 4*B*) (25), consistent with the notion that cargo binding by KLC^{TPR} results in conformational change in KLC. Treatment of cells with 50 μM kinesore caused a comparable reduction in FRET (4.04 ± 0.49%), suggesting that kinesore induces the light-chain conformational switch in a manner similar to activating cargoes.

Discussion

Kinesin family proteins play key roles in both cargo transport on microtubules and in controlling microtubule dynamics to support a wide range of cellular processes (3, 36). Some, such as the kinesin-4 family member Kif21B, possess both of these capacities, which are fine-tuned for its function (37). Is has been appreciated for many years that kinesin-1 also possesses both of these abilities (6). However, the molecular mechanisms that underpin and regulate the balance between these two activities and their relationship to kinesin-1 autoinhibition remain largely unknown. Here we have employed a chemical biology-driven approach to test the hypothesis that these functions are linked through a common regulatory mechanism. Our identification of kinesore as a small molecule that inhibits the SKIP–KLC2 interaction in vitro yet promotes kinesin-1 function in controlling the organization of the microtubule network in cells strongly supports our hypothesis. Moreover, the data provide a proof-of-concept that a microtubule motor–cargo interface and associated autoregulatory mechanism can be manipulated using a small molecule, and defines a potential target for the modulation of microtubule dynamics.

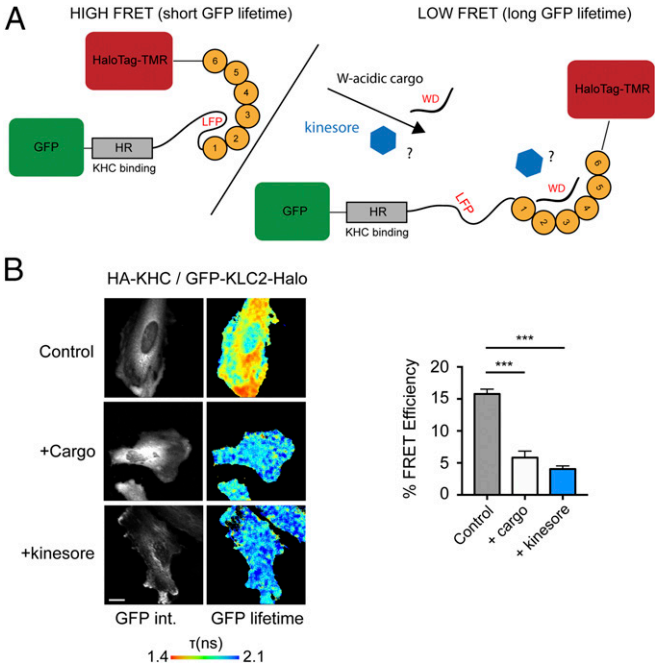

Fig. 4. Kinesore induces the cargo-driven KLC conformational switch. (*A*) Schematic showing KLC2 FRET biosensor with an N-terminal eGFP and a C-terminal HaloTag that allows covalent coupling of TMR. (*Left*) The autoinhibitory interaction mediated by the light chain LFP motif is indicated (25). (*Right*) A representation of the change in conformation to the low FRET state induced by the coexpression of the W-acidic cargo CSTN1. (*B*) Multiphoton fluorescent lifetime images of FRET between GFP and TMR-HaloTag in cells transfected with HA-KHC and GFP-KLC2-Halo biosensor and either cotransfected with CSTN (879–971) (cargo) or treated with 50 μM kinesore for 1 h. "GFP int." are multiphoton GFP intensity images, whereas lifetime image refers to the fluorescence lifetime of GFP (τ) and is represented by a pseudocolor scale. In these images, a reduction in lifetime (change in color from blue to red) indicates FRET and therefore close association of GFP and TMR-HaloTag. Graphs show data from 12 cells from two independent experiments expressed as FRET efficiency. (Scale bar, 10 μm.) FRET is significantly reduced by either cargo cotransfection or 1-h kinesore treatment. Error bars are ± SEM ,$***P <$ 0.001 determined using one-way ANOVA and comparing to control.

Collectively, our data suggest a model in which kinesore engages the KLCs of kinesin-1 in cargo-like fashion to initiate crucial events in cargo-dependent activation, the net result of which is to promote the function of the motor in regulating microtubule bundling and sliding, leading to the remodeling of the microtubule network.

Our favored model builds upon our recent studies (11, 25, 28) and those of others (24, 26), and proposes that in the absence of cargo, kinesin-1 is in its "double autoinhibited" conformations mediated by an intramolecular motor domain–KHC-tail interaction and the KLC^{TPR}–LFP-acidic linker interaction. Kinesin-1 activation is initiated by cargo binding to KLC^{TPR}, resulting in displacement of the LFP-acidic linker region and light-chain conformational change, which in turn leads to destabilization of KHC autoinhibition through a mechanism involving both steric and electrostatic factors (24, 25). One consequence of this is to make accessible a binding site in KHC-tail adjacent to the autoinhibitory IAK sequence. This site is capable of interacting with either organelle cargo adaptors (28) or microtubules (9, 14, 15, 19). Thus, the KLCs gate access to this crucial KHC-tail site. We suggest that kinesore initiates this process while simultaneously inhibiting KLC^{TPR} association with organelle cargo adaptors, forcing kinesin-1 to perform its role in promoting bundling and sliding, resulting in the formation of loops and bundles that bear a notable resemblance to those previously observed following overexpression of an active microtubule sliding kinesin-14 family member (32). Bundling of parallel microtubules and sliding of antiparallel microtubules (6) in the background of continuing plus-end dynamics progressively leads to the emergence of the complex phenotypes observed.

It is worth stating explicitly that we make no claim regarding the specificity of kinesore outside of this limited functional space. Given that the compound must be used at relatively high concentrations in cells (25–50 μM), it is highly likely that other cellular targets exist, although it is unlikely that these make a significant contribution to the microtubule phenotype described. We have not observed any direct effects in vitro on tubulin polymerization, suggesting that this not likely a major component of the cellular activity of kinesore; however, we cannot rule out the possibility of a synergistic direct or indirect activity that combines with the compound's effect on kinesin-1 that is not captured in these assays.

Nonetheless, it is worth reflecting on the proof-of-concept established here. To our knowledge this study is unique in using a small molecule to target the cargo-binding interface and associated autoregulatory mechanism of a cytoskeletal motor. We suggest that this offers several exciting possibilities for the future. Most small molecules that modulate cytoskeletal motor protein function target the ATPase activity or motility mechanisms associated with motor domains that are relatively well conserved within the kinesin, myosin, and dynein families, thus hindering the development of specific functional modulators. In contrast, although autoregulation coupled to cargo recognition represent common themes, the mechanisms by which this is achieved are quite divergent (3, 38–41). For example, kinesin-1 is the only kinesin family member that employs a TPR domain–short linear motif cargo-recognition mechanism (11) that is coupled to its autoregulatory mechanism (25). Indeed, this makes it very unlikely that kinesore has activity against any other kinesin family member. Thus, targeting of these mechanisms may represent an alternative approach to achieving small-molecule control of motor protein function for use as both research tools and for potential therapeutic purposes where motor proteins are dysregulated. Importantly, this approach offers the prospect of not only inhibiting, but also enhancing specific motor protein activities. Developments over recent years establishing the structural basis for cargo recognition and autoregulation are an essential prerequisite for this approach: myosin V, MCAK, cytoplasmic dynein, and dynein-2 all represent potential candidates where structural and biophysical analysis allows one to consider similar in vitro screening-based approaches to target core cargo recognition and autoregulatory mechanisms (38, 39, 42–44). Other candidates and mechanisms in all three families will surely emerge as studies continue to define the molecular underpinnings of these processes.

Finally, it is worth considering the potential of the kinesin-1–cargo interface itself as a drug target. Microtubule targeting agents (stabilizers and destabilizers) represent an important class of chemotherapeutics, but are limited by issues of both toxicity and resistance. Molecules that offer a mechanistically distinct approach to the modulation of microtubule dynamics are actively sought (45). It is conceivable that a molecule that bound the kinesin-1–cargo interface with both high affinity and selectivity, and elicited similar effects to kinesore, could represent such a drug. One might also consider whether manipulation of kinesin-1 activity could be advantageous in neurological conditions where axonal transport is impaired (46). Clearly, therefore, a structural understanding of the kinesore mechanism is imperative, as this would facilitate rational design and phenotypic screening approaches.

Materials and Methods

TR-FRET Assay for the Primary Screen of the 2,908 Compound Pfizer Chemogenomics Small-Molecule Library. The screen was carried out using nonbinding coated 384-well plates with flat-bottomed wells (781900; Corning). Next, 250 nL of 2,908 compounds at 4 mM in DMSO, or DMSO only controls, were supplied prealiquoted in duplicate wells on the same plate. A premade master reaction mix comprising 20 μL of 8 μM Tb-aiKLC2^{TPR}, 10 μM Alexa647-SKIP^{WD} (95% unlabeled peptide, 5% labeled, amino terminally conjugated, sequence STNLEWDDSAI; Biosynthesis Inc) in 25 mM Hepes (pH 7.5), 150 mM NaCl, 5 mM β-ME, was added to each well [giving a final DMSO concentration of 1.25% (vol/vol) and compound

concentration of 49.4 μM]. Plates were incubated at room temperature for 30 min and subsequently analyzed using an Artemis TR-FRET K-101 plate reader (Kyoritsu Radio) at an excitation wavelength of 340 nm, measuring FRET as a ratio of 665-nm (acceptor) to 620-nm (donor) emission intensity, with a time delay of 100 μs following excitation. TR-FRET ratio was normalized to in plate DMSO controls. Compounds that elicited a decrease in TR-FRET ratio that fell outside of a fitting of a normal distribution to the data (50 compounds) were selected for further analysis. Compounds with inconsistent duplicates were disregarded.

Expression, Purification, and Terbium Labeling of aiKLC2^{TPR}. His-KLC2 161–480 (aiKLC2^{TPR}) protein was expressed in BL21 *Escherichia coli*, isolated by nickel-affinity chromatography and further purified by size-exclusion chromatography in 500 mM NaCl, as previously described (25). Ten microliters of 100 μM (1 μmole) purified protein was dialyzed overnight at 4 °C into a labeling buffer comprising 100 mM Na_2CO_3 and 150 mM NaCl at pH 9.3. The protein was labeled with 100 μg (95 nmols) of amine-reactive Terbium chelate (Lanthascreen, PV3582; Thermofisher Scientific) for 3 h at room temperature on a rolling platform, giving a theoretical maximum labeling of ∼1 Tb per 10 aiKLC2^{TPR}. The product of this reaction was subsequently centrifuged at 16,000 × *g* for 20 min and passed through 0.22-μm filter and further purified, removing any free label using a second round of size-exclusion chromatography on a 16/60 HiLoad Superdex 75 column (GE Healthcare), pooling all protein-containing fractions (labeled and unlabeled). The presence of Tb with the characteristic four-peak emission profile in the final pool was confirmed using a fluorimeter following excitation at 340 nm. This mix of labeled and nonlabeled aiKLC2 was then dialyzed overnight at 4 °C into 25 mM Hepes (pH 7.5), 150 mM NaCl, 5 mM β-ME buffer in preparation for use in the TR-FRET screen.

See *SI Materials and Methods* for further discussion.

ACKNOWLEDGMENTS. We thank Professor Anthony Hyman (Max-Planck Institute for Cell Biology and Genetics) for the gift HeLa-Kyoto cell lines; Dr. Rachel Gurrell (Pfizer Ltd) for facilitating access to the Chemogenomics small-molecule library; Dr. Simon Brayford (Kings College London) and the Kings College London Nikon Imaging Centre for assistance with microscopy; Prof. Vladimir Gelfand (Northwestern University), Prof. Ulrike Eggert (Kings College London), and Dr. Anthony Roberts (Birkbeck) for providing helpful discussions on the project; and Prof. Anne Ridley (Kings College London) for critical reading of the manuscript. This work was funded by Wellcome Trust Research Career Development Fellowship 097316/Z/11/Z (to M.P.D.). Y.Y.Y. is supported by Biotechnology and Biological Sciences Research Council project Grant BB/L006774/1 (to M.P.D. and R.A.S.). K.P. and M.P. were supported by UK Medical Research Council Grant MR/K015664/1. A.J.B. was supported by Asthma UK (09/029).

1. Vale RD (2003) The molecular motor toolbox for intracellular transport. *Cell* 112: 467–480.
2. Vale RD, Reese TS, Sheetz MP (1985) Identification of a novel force-generating protein, kinesin, involved in microtubule-based motility. *Cell* 42:39–50.
3. Verhey KJ, Hammond JW (2009) Traffic control: Regulation of kinesin motors. *Nat Rev Mol Cell Biol* 10:765–777.
4. Fu M-M, Holzbaur ELF (2014) Integrated regulation of motor-driven organelle transport by scaffolding proteins. *Trends Cell Biol* 24:564–574.
5. Jolly AL, et al. (2010) Kinesin-1 heavy chain mediates microtubule sliding to drive changes in cell shape. *Proc Natl Acad Sci USA* 107:12151–12156.
6. Lu W, Gelfand VI (2017) Moonlighting motors: Kinesin, dynein, and cell polarity. *Trends Cell Biol* 27:505–514.
7. Urrutia R, McNiven MA, Albanesi JP, Murphy DB, Kachar B (1991) Purified kinesin promotes vesicle motility and induces active sliding between microtubules in vitro. *Proc Natl Acad Sci USA* 88:6701–6705.
8. Andrews SB, Gallant PE, Leapman RD, Schnapp BJ, Reese TS (1993) Single kinesin molecules crossbridge microtubules in vitro. *Proc Natl Acad Sci USA* 90:6503–6507.
9. Straube A, Hause G, Fink G, Steinberg G (2006) Conventional kinesin mediates microtubule-microtubule interactions in vivo. *Mol Biol Cell* 17:907–916.
10. Lu W, Lakonishok M, Gelfand VI (2015) Kinesin-1-powered microtubule sliding initiates axonal regeneration in *Drosophila* cultured neurons. *Mol Biol Cell* 26: 1296–1307.
11. Pernigo S, Lamprecht A, Steiner RA, Dodding MP (2013) Structural basis for kinesin-1: Cargo recognition. *Science* 340:356–359.
12. Verhey KJ, et al. (2001) Cargo of kinesin identified as JIP scaffolding proteins and associated signaling molecules. *J Cell Biol* 152:959–970.
13. Blasius TL, Cai D, Jih GT, Toret CP, Verhey KJ (2007) Two binding partners cooperate to activate the molecular motor kinesin-1. *J Cell Biol* 176:11–17.
14. Navone F, et al. (1992) Cloning and expression of a human kinesin heavy chain gene: Interaction of the COOH-terminal domain with cytoplasmic microtubules in transfected CV-1 cells. *J Cell Biol* 117:1263–1275.
15. Seeger MA, Rice SE (2010) Microtubule-associated protein-like binding of the kinesin-1 tail to microtubules. *J Biol Chem* 285:8155–8162.
16. Kaan HYK, Hackney DD, Kozielski F (2011) The structure of the kinesin-1 motor-tail complex reveals the mechanism of autoinhibition. *Science* 333:883–885.
17. Dietrich KA, et al. (2008) The kinesin-1 motor protein is regulated by a direct interaction of its head and tail. *Proc Natl Acad Sci USA* 105:8938–8943.
18. Hackney DD, Baek N, Snyder AC (2009) Half-site inhibition of dimeric kinesin head domains by monomeric tail domains. *Biochemistry* 48:3448–3456.
19. Hackney DD, Stock MF (2000) Kinesin's IAK tail domain inhibits initial microtubule-stimulated ADP release. *Nat Cell Biol* 2:257–260.
20. Friedman DS, Vale RD (1999) Single-molecule analysis of kinesin motility reveals regulation by the cargo-binding tail domain. *Nat Cell Biol* 1:293–297.
21. Stock MF, et al. (1999) Formation of the compact confomer of kinesin requires a COOH-terminal heavy chain domain and inhibits microtubule-stimulated ATPase activity. *J Biol Chem* 274:14617–14623.
22. Coy DL, Hancock WO, Wagenbach M, Howard J (1999) Kinesin's tail domain is an inhibitory regulator of the motor domain. *Nat Cell Biol* 1:288–292.
23. Verhey KJ, et al. (1998) Light chain-dependent regulation of kinesin's interaction with microtubules. *J Cell Biol* 143:1053–1066.
24. Wong YL, Rice SE (2010) Kinesin's light chains inhibit the head- and microtubule-binding activity of its tail. *Proc Natl Acad Sci USA* 107:11781–11786.
25. Yip YY, et al. (2016) The light chains of kinesin-1 are autoinhibited. *Proc Natl Acad Sci USA* 113:2418–2423.
26. Kawano T, et al. (2012) A small peptide sequence is sufficient for initiating kinesin-1 activation through part of TPR region of KLC1. *Traffic* 13:834–848.
27. Dodding MP, Mitter R, Humphries AC, Way M (2011) A kinesin-1 binding motif in vaccinia virus that is widespread throughout the human genome. *EMBO J* 30:4523–4538.
28. Sanger A, et al. (2017) SKIP controls lysosome positioning using a composite kinesin-1 heavy and light chain-binding domain. *J Cell Sci* 130:1637–1651.
29. Lee TJ, Lee JW, Haynes EM, Eliceiri KW, Halloran MC (2017) The kinesin adaptor calsyntenin-1 organizes microtubule polarity and regulates dynamics during sensory axon arbor development. *Front Cell Neurosci* 11:107.
30. Nikolovska-Coleska Z, et al. (2004) Development and optimization of a binding assay for the XIAP BIR3 domain using fluorescence polarization. *Anal Biochem* 332:261–273.
31. Rosa-Ferreira C, Munro S (2011) Arl8 and SKIP act together to link lysosomes to kinesin-1. *Dev Cell* 21:1171–1178.
32. Oladipo A, Cowan A, Rodionov V (2007) Microtubule motor Ncd induces sliding of microtubules in vivo. *Mol Biol Cell* 18:3601–3606.
33. Maliga Z, et al. (2013) A genomic toolkit to investigate kinesin and myosin motor function in cells. *Nat Cell Biol* 15:325–334.
34. Tanaka Y, et al. (1998) Targeted disruption of mouse conventional kinesin heavy chain, kif5B, results in abnormal perinuclear clustering of mitochondria. *Cell* 93: 1147–1158.
35. Essletzbichler P, et al. (2014) Megabase-scale deletion using CRISPR/Cas9 to generate a fully haploid human cell line. *Genome Res* 24:2059–2065.
36. Cross RA, McAinsh A (2014) Prime movers: The mechanochemistry of mitotic kinesins. *Nat Rev Mol Cell Biol* 15:257–271.
37. Ghiretti AE, et al. (2016) Activity-dependent regulation of distinct transport and cytoskeletal remodeling functions of the dendritic kinesin KIF21B. *Neuron* 92:857–872.
38. Li J, Lu Q, Zhang M (2016) Structural basis of cargo recognition by unconventional myosins in cellular trafficking. *Traffic* 17:822–838.
39. Zhang K, et al. (2017) Cryo-EM reveals how human cytoplasmic dynein is auto-inhibited and activated. *Cell* 169:1303–1314.e18.
40. McKenney RJ, Huynh W, Tanenbaum ME, Bhabha G, Vale RD (2014) Activation of cytoplasmic dynein motility by dynactin-cargo adapter complexes. *Science* 345: 337–341.
41. Schlager MA, Hoang HT, Urnavicius L, Bullock SL, Carter AP (2014) In vitro reconstitution of a highly processive recombinant human dynein complex. *EMBO J* 33: 1855–1868.
42. Wei Z, Liu X, Yu C, Zhang M (2013) Structural basis of cargo recognitions for class V myosins. *Proc Natl Acad Sci USA* 110:11314–11319.
43. Toropova K, Mladenov M, Roberts AJ (2017) Intraflagellar transport dynein is autoinhibited by trapping of its mechanical and track-binding elements. *Nat Struct Mol Biol* 24:461–468.
44. Talapatra SK, Harker B, Welburn JPI (2015) The C-terminal region of the motor protein MCAK controls its structure and activity through a conformational switch. *eLife* 4: e06421.
45. Dumontet C, Jordan MA (2010) Microtubule-binding agents: A dynamic field of cancer therapeutics. *Nat Rev Drug Discov* 9:790–803.
46. Goldstein LSB (2012) Axonal transport and neurodegenerative disease: Can we see the elephant? *Prog Neurobiol* 99:186–190.